



Superconducting pairing symmetries of the Hubbard model on the honeycomb lattice with inhomogeneous hopping strength

Tao Ying  and Shuhui Yang*School of Physics, Harbin Institute of Technology, Harbin 150001, China* (Received 2 June 2020; revised 3 September 2020; accepted 3 September 2020; published 16 September 2020)

Using finite-temperature determinantal quantum Monte Carlo calculations, we find that the dominant pairing symmetries in the standard Hubbard model on the honeycomb lattice depend on the electron filling. When the electron density ρ is larger than around 0.25, the dominant pairing symmetry is the $d + id$ -wave; when the electron density is low enough ($\rho \lesssim 0.25$), the dominant pairing symmetry is the $p + ip$ wave. For two electron densities $\rho = 0.1$ and $\rho = 0.4$, where the dominant pairing symmetries are $p + ip$ wave and $d + id$ wave separately, we study the effect of two types of hopping inhomogeneities (the plaquette and the quasi-1D hopping inhomogeneities) on the pairing symmetries. For $\rho = 0.1$, the plaquette hopping inhomogeneity drives the dominant $p + ip$ -wave pairing symmetry into the $d + id$ -wave; while the quasi-1D hopping inhomogeneity almost does not affect the $p + ip$ wave, and arises the f wave, causing the coexistence of $p + ip$ -wave and f -wave pairing. For $\rho = 0.4$, both the plaquette and the quasi-1D hopping inhomogeneities destroy the $d + id$ -wave pairing symmetry, without causing other pairing symmetry. Our results suggest that the effect of hopping inhomogeneity on the pairing symmetries is robust and depends on the electron filling. This finding may be useful for the design of artificial graphene superconductors with different kinds of pairing, especially for the realization of the $d + id$ -wave, $p + ip$ -wave, or f -wave superconductors at low filling.

DOI: [10.1103/PhysRevB.102.125125](https://doi.org/10.1103/PhysRevB.102.125125)

I. INTRODUCTION

Graphene is among the most interesting novel materials due to its fascinating electronic properties [1]. Undoped graphene is expected to have a strong correlated effect due to its massless Dirac fermion spectrum and the nontrivial two-dimensional honeycomb structure [2]. When doped, more exotic phases such as magnetism, charge density wave, spin density wave, and superconducting instabilities are proposed theoretically [3–11], though many of them have not been experimentally observed yet. Most of those studies are based on the standard Hubbard model on the honeycomb lattice, among which the exploration of the unconventional superconductivity is being very actively pursued [12]. So far, most of the theoretical studies propose the possibility of $d + id$ -wave superconductivity in doped graphene [6,13–20], with some other studies suggesting the (co)existence of extended s -wave, $p + ip$ -wave, and even f -wave pairing symmetries [6,18,19,21,22]. More recently, the pairing symmetries on the Hubbard honeycomb lattice as functions of electron filling, interaction strength, and temperature were systematically studied using a quantum Monte Carlo algorithm [23], which also argues a $d + id$ -wave pairing symmetry in most parameter regions. But the pairing symmetries at pretty low electron filling have not been studied.

On the other side, recently it became possible to fabricate graphene [24]. This motivates people to seek exotic quantum phases on an inhomogeneous Hubbard honeycomb lattice [25–28]. A typical inhomogeneous Hubbard model on the honeycomb lattice is the one with inhomogeneous hopping

strength, which can be easily realized such as in strained graphene. So it will be interesting to study how the hopping inhomogeneity affects the pairing symmetries on the Hubbard honeycomb lattice. Two types of hopping inhomogeneities are of great research interests. The first one is the so-called “plaquette” hopping inhomogeneity, for which several single hexagons with hopping t are connected by hopping t' to form the honeycomb structure (cf. Fig. 4). The original idea of this plaquette hopping inhomogeneity was generated on a Hubbard square lattice, i.e., a square lattice consisting of a periodic array of 2×2 plaquettes with hopping t connected by a weaker hybridization t' . The presence of inhomogeneous hoppings introduces many new phases [29]. A key question is whether some intermediate t' will cause optimal electron pairing. Some studies suggest that such an ‘optimal inhomogeneity’ does exist [30–32], while some studies give the negative answer [33,34]. Though the existence of the ‘optimal inhomogeneity’ on the Hubbard square lattice is still controversial, it is worth it to extend such a question to the honeycomb lattice. Even on an isotropic honeycomb lattice, the theoretical studies based on the Hubbard or Heisenberg model predict the formation of the plaquette order [35–38]. So it will be interesting to see, if we enforce the plaquette structure, how the properties of the system will be affected. Since nowadays people can manipulate 2D artificial atomic crystals easily [24], such a synthetic plaquette honeycomb structure has already been designed for studying unconventional superconductivity, electron fractionalization, massless Dirac quasiparticles and their topological and correlated phases [5,39–41].

The second type of hopping inhomogeneity is motivated from strained graphene, a honeycomb lattice built from zigzag lines with hopping t connected by t' (cf. Fig. 8). In the following we will call this type of hopping inhomogeneity the quasi-1D hopping inhomogeneity, since the lattice becomes 1D when t' reduces to 0. The quasi-1D hopping inhomogeneity is interesting because it can tune the hopping strengths and can be realized experimentally, such as through nanopatterning, molecule-by-molecule assembly, trapping ultracold atoms on optical lattices, or application of strain [28,40,42]. This inhomogeneous honeycomb lattice geometry can also be taken as the 1/3-depleted square lattice [28], connecting directly with the layered nickelates $\text{La}_4\text{Ni}_3\text{O}_8$ and $\text{La}_3\text{Ni}_2\text{O}_6$, which have been studied recently, both theoretically [43] and experimentally [44].

Based on the discussion above, we first extend the study of the pairing symmetries on the Hubbard honeycomb lattice into low electron filling, to explore which pairing channel is dominant in that region. Then we study the effect of the plaquette and the quasi-1D hopping inhomogeneities on the pairing symmetries. The rest of the paper is organized as follows: In Sec. II, we introduce the Hubbard Hamiltonian with inhomogeneous hopping t' and outline our quantum Monte Carlo approach to calculate the effective pairing susceptibility in different pairing channels. In Sec. III we first calculate the dominant pairing symmetries at low electron density region, then study how those two types of hopping inhomogeneities affect the pairing symmetries. Finally, we summarize the main conclusion in Sec. IV.

II. HAMILTONIAN AND METHODOLOGY

The standard model to study the pairing symmetries on graphene is the Hubbard model on the honeycomb lattice. With the introduction of the hopping inhomogeneity, this model Hamiltonian can be written as:

$$\begin{aligned} \hat{H} = & -t \sum_{(ij) \in \mathcal{P}, \sigma} (c_{i\sigma}^\dagger c_{j\sigma} + c_{j\sigma}^\dagger c_{i\sigma}) \\ & -t' \sum_{(ij) \notin \mathcal{P}, \sigma} (c_{i\sigma}^\dagger c_{j\sigma} + c_{j\sigma}^\dagger c_{i\sigma}) \\ & + U \sum_i \left(n_{i\uparrow} - \frac{1}{2} \right) \left(n_{i\downarrow} - \frac{1}{2} \right) - \mu \sum_i (n_{i\uparrow} + n_{i\downarrow}). \end{aligned} \quad (1)$$

Here $c_{i\sigma}^\dagger$ ($c_{i\sigma}$) are the creation (destruction) operators for fermions of spin σ on lattice site i . U is the onsite repulsive interaction. μ is the chemical potential to tune the electron density, which is the average number of the total electrons on a finite lattice. The nearest-neighbor (NN) sites $(ij) \in \mathcal{P}$ are connected by hopping t , while $(ij) \notin \mathcal{P}$ denotes NN sites i, j connected by hopping t' . Two types of hopping inhomogeneities, the plaquette and the quasi-1D hopping inhomogeneities, are specified in Fig. 4 and Fig. 8 separately. The interaction term is written into particle-hole symmetric form, so that $\mu = 0$ corresponds to half filling, even with the presence of the hopping inhomogeneity. We set $t = 1$ to set the energy scale, while t' varies from 0 to 1.

Our methodology is the finite-temperature determinantal quantum Monte Carlo (FT-DQMC) [45,46]. In FT-DQMC, the expectation values of observables $\langle \hat{M} \rangle = \text{Tr} \hat{M} \exp(-\beta \hat{H}) / \text{Tr} \exp(-\beta \hat{H})$ are evaluated by discretizing the inverse temperature β and rewriting the partition function as a path integral. To integrate out the fermion degrees of freedom analytically, one needs to do a Hubbard-Stratonovich (HS) transformation to write the interaction term of the Hubbard Hamiltonian into the quadratic term; the price is the introduction of the HS auxiliary field. Then what is left is the classic Monte Carlo calculation of the auxiliary field. The product of fermion determinants (one determinant for each spin species) performs as the weight to sample the auxiliary field. For most cases, the product of the two fermion determinants is not guaranteed to be positive for all configurations, which causes the sign problem [47]. At half filling, because spatial variations in the hopping do not destroy particle-hole symmetry, there is no sign problem. But for the doping case, the sign problem arises and gets worse upon lowering temperature T and increasing interaction strength U , which will temper our ability to make conclusive statements about the pairing symmetries at low enough T .

To look at the pairing symmetries, we calculate the pairing susceptibilities of the above Hamiltonian:

$$\chi_\alpha = \frac{1}{N_s} \sum_{\mathbf{i}, \mathbf{j}} \int_0^\beta d\tau \langle \Delta_{\alpha\mathbf{i}}^\dagger(\tau) \Delta_{\alpha\mathbf{j}}(0) \rangle \quad (2)$$

with the order parameter

$$\begin{aligned} \Delta_{\alpha\mathbf{i}}^\dagger(\tau) &= e^{\tau H} \Delta_{\alpha\mathbf{i}}^\dagger(0) e^{-\tau H} \\ \Delta_{\alpha\mathbf{i}}^\dagger(0) &= \frac{1}{\sqrt{N_l}} \sum_l f_\alpha^\dagger(\delta_l) (c_{i\uparrow} c_{i+\delta_l\downarrow} \pm c_{i\downarrow} c_{i+\delta_l\uparrow})^\dagger. \end{aligned} \quad (3)$$

Here α means the different pairing channels; in this paper we consider the NN extended s -wave, NN $d + id$ -wave, and NN $p + ip$ -wave pairing symmetries, and the next-nearest-neighbor (NNN) $d + id$ -wave, NNN $p + ip$ -wave and NNN f -wave pairing symmetries. f_α is the form factor of the α pairing function, $f_{\text{NN},es}(\delta_l) = 1$, $f_{\text{NN},d+id}(\delta_l) = e^{i(l-1)\frac{2\pi}{3}}$, $f_{\text{NN},p+ip}(\delta_l) = e^{i(l-1)\frac{2\pi}{3} + \epsilon_s i\pi}$, $f_{\text{NNN},d+id}(\delta_l') = e^{i(l-1)\frac{2\pi}{3}}$, $f_{\text{NNN},p+ip}(\delta_l') = e^{i(l-1)\frac{\pi}{3}}$, $f_{\text{NNN},f}(\delta_l') = e^{i\frac{1+(-1)^l}{2}\pi}$. The vectors δ_l denote different pairing connections and N_l is the normalization parameter, so with NN pairing, $l = 1, 2, 3$, $N_l = 3$, while for NNN pairing, $l = 1, 2, 3, 4, 5, 6$, $N_l = 6$. ϵ_s equals 0 (1) for sites on the A (B) sublattice. In Eq. (3), $+$ and $-$ denote triplet and singlet states, respectively. Our calculations are for finite inverse temperature $\beta = 1/T$ and on finite lattice size $N_s = L \times L \times 2$.

To extract the effective pairing vertex [48], we also need to calculate the bare pairing susceptibility $\tilde{\chi}_\alpha$ using FT-DQMC. For the calculation of $\tilde{\chi}_\alpha$, the terms $\langle c_{i\downarrow}^\dagger(\tau) c_{j\downarrow}(0) c_{\mathbf{k}\uparrow}^\dagger(\tau) c_{\mathbf{l}\uparrow}(0) \rangle$ that appear in χ_α in Eq. (2) are replaced by the decoupled contributions $\langle c_{i\downarrow}^\dagger(\tau) c_{j\downarrow}(0) \rangle \langle c_{\mathbf{k}\uparrow}^\dagger(\tau) c_{\mathbf{l}\uparrow}(0) \rangle$. The effective pairing susceptibilities are then given as $\chi_\alpha^{\text{eff}} = \chi_\alpha - \tilde{\chi}_\alpha$. When χ_α^{eff} is positive, it signals a favorable pairing symmetry in the α channel, while a negative χ_α^{eff} means the α pairing channel is unfavorable.

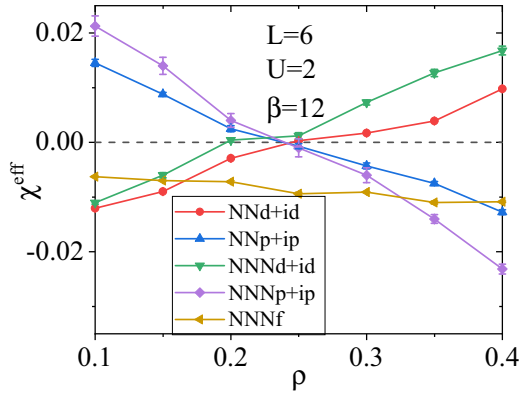


FIG. 1. Effective pairing susceptibilities χ^{eff} as functions of electron density ρ , on a $6 \times 6 \times 2$ lattice, $U = 2$ and $\beta = 12$. With the decrease of ρ , the dominant pairing channel changes from $d + id$ wave to $p + ip$ wave.

III. RESULTS

A. The homogeneous case

We start from the homogeneous hopping case $t' = t = 1$, where the pairing symmetries on the honeycomb lattice are extensively studied from the intermediate to high electron density region, and it's generally accepted that the $d + id$ -wave pairing is the dominant pairing symmetry. Here we extend the study to the low-filling region, from $\rho = 0.4$ to $\rho = 0.1$. The effective pairing susceptibilities χ^{eff} as functions of electron density ρ are shown in Fig. 1, for $L = 6$, $U = 2$, and $\beta = 12$. It is clear that when electron density is relatively high ($\rho \gtrsim 0.25$), the dominant pairing is $d + id$ wave; when the electron density is low enough ($\rho \lesssim 0.25$), it is interesting that the dominant pairing symmetry switches to $p + ip$ wave. We clarify that in all the cases considered in this paper, the effective extended s -wave pairing susceptibility is always negative (and its absolute value is much larger than the data in other pairing channels), meaning the extended s -wave pairing is always unfavorable. So we will not show the data of extended s -wave pairing, to make the plots more readable. As can be seen from Fig. 1 and the other figures in this paper, the behavior of the NN $d + id$ (and $p + ip$) pairing symmetries always agree with the NNN ones. So in the following, we will ignore the notation NN or NNN.

The results shown in Fig. 1 depend on the linear finite lattice size L , the finite temperature T , and the interaction strength U . So we need to consider whether our results depend qualitatively on the values of those parameters. We look at this problem for $\rho = 0.4$ and $\rho = 0.1$ which correspond to the dominant $d + id$ wave and dominant $p + ip$ wave separately. We first look at the finite temperature effect by lowering the value of T . One needs to note that the relationship between electron density ρ and chemical potential μ is sensitive to the parameters such as T , U , or t' . So when the parameters change, we need to tune the chemical potential to keep the electron density fixed. When the temperature is high, χ^{eff} in all pairing channels is close to 0, suggesting the quantum effect is ignorable due to high temperature. With the decrease of T , as shown in Fig. 2, it is clear that the dominant effective pairing susceptibilities increase and diverge when T is low

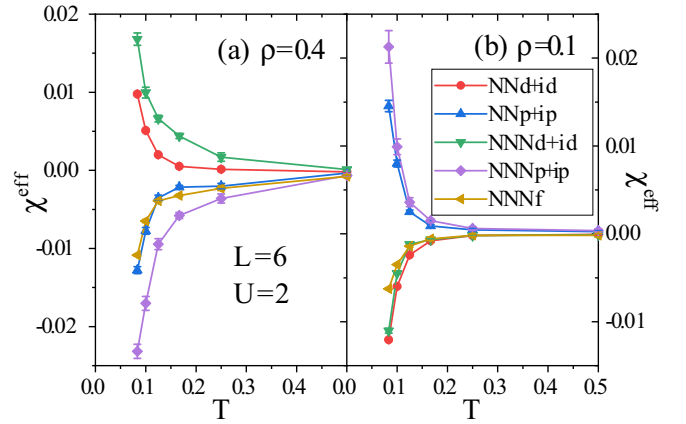


FIG. 2. On a $6 \times 6 \times 2$ lattice and $U = 2$, effective pairing susceptibilities χ^{eff} as functions of temperature T , for (a) $\rho = 0.4$ and (b) $\rho = 0.1$. With the decrease of T , the dominant pairing susceptibility diverges significantly.

enough ($d + id$ wave for $\rho = 0.4$ and $p + ip$ wave for $\rho = 0.1$), while the unfavorable effective pairing susceptibilities become negative significantly ($p + ip$ wave and f wave for $\rho = 0.4$, $d + id$ -wave and f wave for $\rho = 0.1$). This result suggests that we need a relatively low T , then the value of T doesn't change the conclusion qualitatively. So the result shown in Fig. 1 stands qualitatively for all low T , and in the following, we will use a suitable $\beta = 12$.

We then check the finite size effect by varying the value of L . Figure 3 shows the effective pairing susceptibilities χ^{eff} in all pairing channels for several lattice sizes $L = 6, 8, 10$, and 12 . χ^{eff} at $\beta = 12$ exhibits clear finite size effect. With the increase of the lattice size, the absolute values of χ^{eff} in all pairing channels decrease. However, this finite size effect doesn't affect the repulsiveness or attractiveness of the effective pairing susceptibilities χ^{eff} , i.e., the favorable or unfavorable pairing symmetries can be obtained from any of the finite lattice sizes. So in the following, we only show the data for one lattice size $L = 6$.

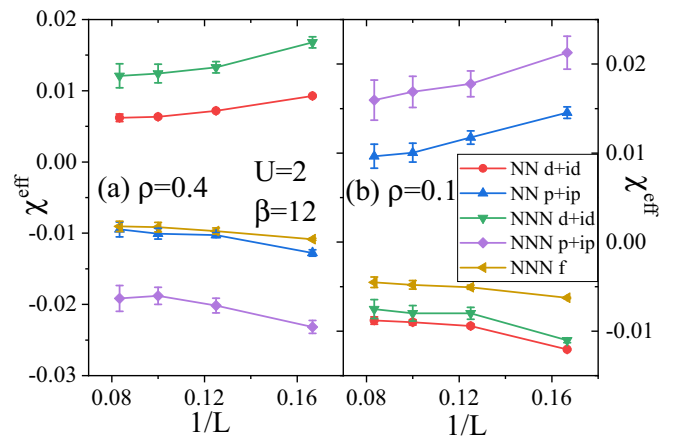


FIG. 3. Effective pairing susceptibilities χ^{eff} as functions of inverse linear lattice size $1/L$, for $U = 2$, $\beta = 12$, (a) $\rho = 0.4$ and (b) $\rho = 0.1$. The finite size effect of χ^{eff} is obvious, but the repulsiveness or attractiveness of χ^{eff} is not affected.

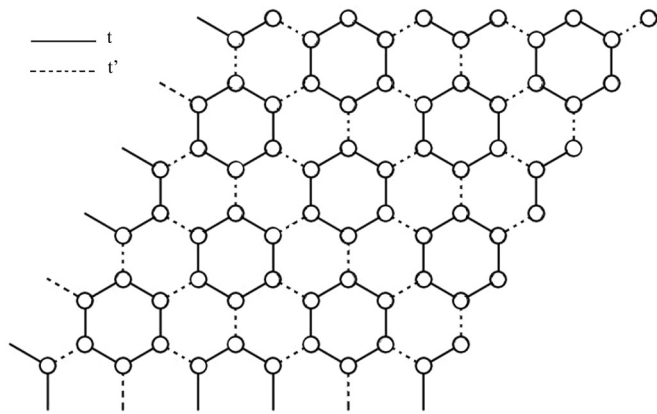


FIG. 4. Lattice geometry for the plaquette Hubbard model, a 2D honeycomb lattice built from plaquettes of strong hopping t connected by weaker hopping t' .

For the homogeneous Hubbard model on honeycomb lattice at half filling, there is a semimetal to antiferromagnetic Mott insulator transition at $U \approx 3.76$. However, as has been studied previously [19,20], the pairing symmetries are not highly sensitive to the ground state, i.e., the dominant pairing symmetry is unchanged for different interaction strengths U . We will see that this argument still stands with the presence of hopping inhomogeneities (Fig. 6 and Fig. 9).

In the following, we will focus on the two electron densities $\rho = 0.1$ and $\rho = 0.4$, for which the dominant pairing symmetries in the homogeneous hopping case are $d + id$ wave and $p + ip$ wave separately. Our purpose is to look at how the inhomogeneous hopping affects the dominant pairing symmetries, for both the plaquette case and the quasi-1D case.

B. The plaquette case

The plaquette type of hopping inhomogeneity is shown in Fig. 4. The solid lines denote the standard hopping strength $t = 1$, while the dashed lines mean the weaker hopping

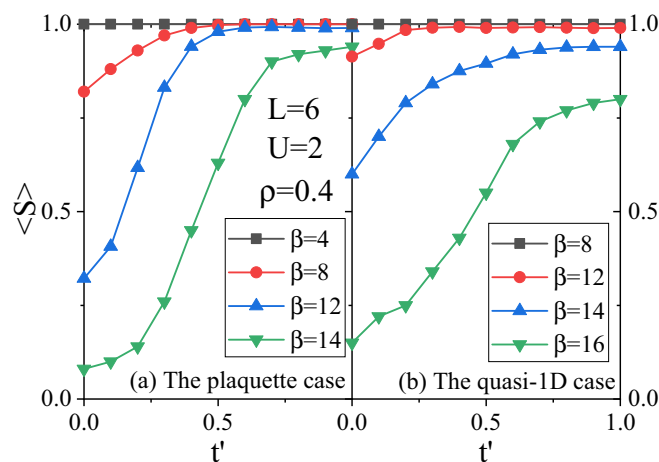


FIG. 5. The average sign $\langle S \rangle$ as a function of t' on a $6 \times 6 \times 2$ lattice, $U = 2$, $\rho = 0.4$ and several temperatures, for both (a) the plaquette case and (b) the quasi-1D case. The decrease of t' apparently worsens the sign problem.

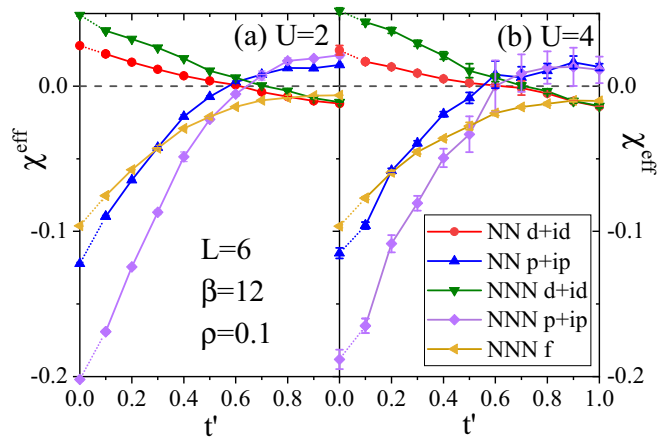


FIG. 6. Effective pairing susceptibilities χ^{eff} as functions of t' , on a $6 \times 6 \times 2$ lattice, $\beta = 12$, $\rho = 0.1$, for (a) $U = 2$ and (b) $U = 4$. With the decrease of t' , the dominant pairing changes from $p + ip$ wave to $d + id$ wave.

strength t' which varies from 1 to 0. Our purpose is to look at how the plaquette hopping inhomogeneity affects the dominant pairing symmetries ($d + id$ wave for $\rho = 0.4$ and $p + ip$ wave for $\rho = 0.1$).

For the FT-DQMC calculations of the Hubbard model away from half filling, the sign problem appears. When the electron density is low, the sign problem is not very severe. However, the hopping inhomogeneity worsens the sign problem, as shown in Fig. 5. Normally for the imaginary-time measurements, we need to have the average sign $\langle S \rangle$ be larger than 0.3, to make sure the numerical accuracy is controllable. With the decrease of the temperature, the value of $\langle S \rangle$ decreases as expected. For $\beta = 12$ which is used for most of the simulations, the worst sign problem is shown in Fig. 5(a) for $t' = 0$, which is slightly larger than 0.3. So all the data in this paper is accurate within error bars.

We first look at the electron density $\rho = 0.1$, where the dominant pairing symmetry is $p + ip$ wave for the homogeneous hopping $t' = t$. As shown in Fig. 6(a) for $U = 2$, the $p + ip$ -wave ($d + id$ -wave) effective pairing susceptibility at $t' = 1$ is positive (negative). With the decrease of t' , the value of χ_{p+ip}^{eff} reduces and becomes negative at $t' \approx 0.6$, while χ_{d+id}^{eff} behaves in the opposite direction. The results suggest that the plaquette type of hopping inhomogeneity suppresses the $p + ip$ -wave pairing and enhances the $d + id$ -wave pairing symmetry. For $t' \lesssim 0.6$, the dominant pairing channel switches from $p + ip$ wave to $d + id$ wave. When t' reduces to 0, the system is broken into a collection of disconnected hexagons, which is equivalent to a six-site 1D system with periodic boundary condition. Even for finite but small enough t' , the system would behave more like 1D, so one might expect a dimensional crossover from 2D to 1D when t' reduces, as has been previously studied focusing on the magnetic properties based on the anisotropic square Hubbard model [49–51]. The pairing symmetries on 1D systems will be qualitatively different from those on the 2D systems. However, due to the complexity of the imaginary-time measurement χ and the sign problem in DQMC calculations, it is difficult to judge numerically whether there is a dimension crossover and its

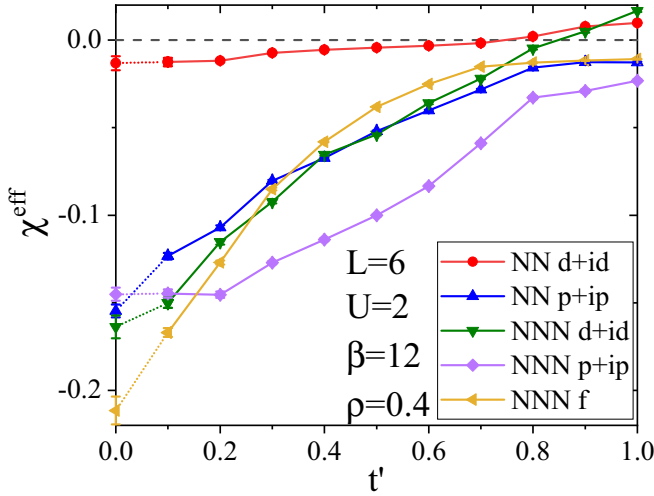


FIG. 7. Effective pairing susceptibilities χ^{eff} as functions of t' , on a $6 \times 6 \times 2$ lattice, $\beta = 12$, $\rho = 0.4$, and $U = 2$. With the decrease of t' , the dominant $d + id$ -wave pairing vanishes, with no other pairing channels aroused.

effect on the pairing information. On the other hand, our numerical calculations for all t' are in the same way, just the value of t' varies, so the data at $t' = 0$ in Fig. 6 (and similarly in Fig. 7, Fig. 9, and Fig. 10) may not reveal the true pairing in a 1D system. We still present the data at $t' = 0$ but use dashed lines to connect the data points for $t' = 0.1$ and $t' = 0$. In Fig. 6(b), we change the value of U to be 4, which gives qualitatively the same result with $U = 2$, supporting the argument that the pairing symmetries are not sensitive to the interaction strength U , even with the presence of the hopping inhomogeneity. Then for the electron density $\rho = 0.4$, where the dominant pairing symmetry is $d + id$ wave for the homogeneous hopping $t' = t$, we check how the plaquette type of hopping inhomogeneity affects the pairing symmetry. Since we have proven the choice of the value of U does not affect the results qualitatively, here we only choose one interaction strength $U = 2$. The data in Fig. 7 show that the dominant $d + id$ -wave pairing symmetry is suppressed by the decrease

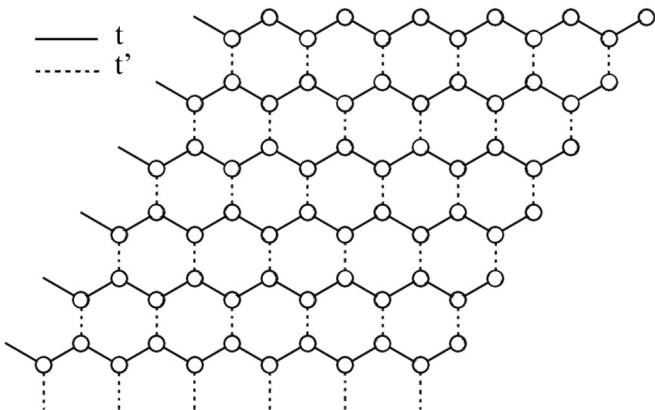


FIG. 8. Lattice geometry for the quasi-1D Hubbard model, a 2D honeycomb lattice built from zigzag line of strong hopping t connected by weaker hopping t' .

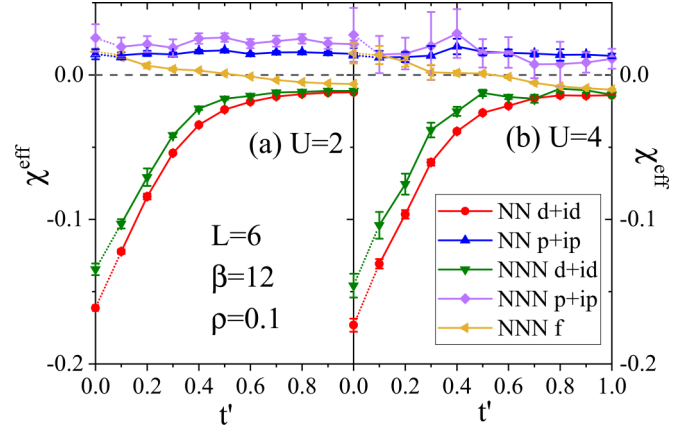


FIG. 9. Effective pairing susceptibilities χ^{eff} as functions of t' , on a $6 \times 6 \times 2$ lattice, $\beta = 12$, $\rho = 0.1$, for (a) $U = 2$ and (b) $U = 4$. With the decrease of t' , the dominant $p + ip$ wave is almost not affected, while the f wave arises slowly, causing the coexistence of $p + ip$ -wave and f -wave pairing.

of t' , with no other pairing symmetries aroused. This means that, for $\rho = 0.4$ and small enough t' , there is no pairing symmetry that persists with the plaquette type of hopping inhomogeneity.

C. The quasi-1D case

The second type of hopping inhomogeneity we considered is shown in Fig. 8; the decrease of the value of t' will drive the honeycomb lattice into individual 1D chains, so we call it the quasi-1D hopping inhomogeneity. For the electron density $\rho = 0.1$ where the dominant pairing symmetry is $p + ip$ wave when $t' = t$, we show in Fig. 9(a) the effect of the quasi-1D hopping inhomogeneity on the pairing symmetries for $U = 2$. The dominant $p + ip$ -wave pairing symmetry is almost unaffected by the decrease of t' , in the meantime, the f -wave effective pairing susceptibility becomes positive, suggesting

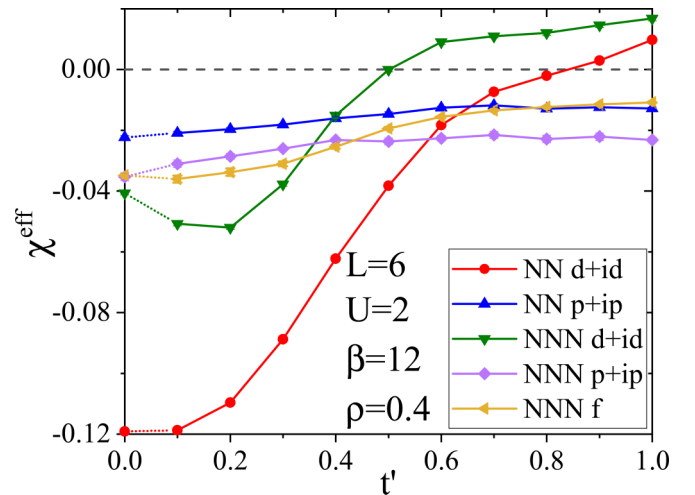


FIG. 10. Effective pairing susceptibilities χ^{eff} as functions of t' , on a $6 \times 6 \times 2$ lattice, $\beta = 12$, $\rho = 0.4$, and $U = 2$. With the decrease of t' , the dominant $d + id$ -wave pairing vanishes, and no other pairing channels appear.

that the quasi-1D hopping inhomogeneity causes the coexistence of the $p + ip$ -wave and the f -wave pairing symmetries. The $U = 4$ data shown in Fig. 9(b) are qualitatively the same with $U = 2$, which again suggest that the pairing symmetries on the honeycomb lattice are not sensitive to the interaction strength U , similar to the homogeneous hopping case [20] and the plaquette hopping inhomogeneity case discussed above.

For the electron density $\rho = 0.4$, we find that the dominant $d + id$ -wave pairing symmetry at $t' = t$ is suppressed by the decrease of t' , and no other pairing symmetries are aroused, as shown in Fig. 10. This is similar to the effect of the plaquette hopping inhomogeneity shown in Fig. 7. This result suggests that when the dominant pairing symmetry in the homogeneous case is $d + id$ wave, there will be no pairing symmetry when the quasi-1D hopping inhomogeneity becomes strong enough.

IV. CONCLUSIONS AND DISCUSSIONS

In this paper, we first extend the previous study of the pairing symmetries on the Hubbard honeycomb lattice into the low electron filling region. Our unbiased FT-DQMC simulations reveal that for electron densities larger than around 0.25, the dominant pairing symmetry is $d + id$ wave; while for smaller electron density ($\rho \lesssim 0.25$), the dominant pairing symmetry is $p + ip$ wave.

Then we study the effect of the plaquette hopping inhomogeneity and the quasi-1D hopping inhomogeneity on the pairing symmetries. When the dominant pairing symmetry at $t = t'$ is $d + id$ wave, both the plaquette hopping inhomogeneity and the quasi-1D hopping inhomogeneity destroy the $d + id$ wave, without causing other pairing symmetry. When the dominant pairing symmetry at $t = t'$ is $p + ip$ wave, the plaquette hopping inhomogeneity destroys the $p + ip$ wave and drives the dominant pairing symmetry into the $d + id$ wave, while the quasi-1D hopping inhomogeneity almost does not affect the $p + ip$ wave, and arises the f

wave, causing the coexistence of $p + ip$ -wave and f -wave pairing.

The understanding of the physical mechanism of the pairing and its evolution with hopping inhomogeneities is quite challenging. It was argued that the $d + id$ -wave pairing normally arises from doping an antiferromagnetic insulator, while the ferromagneticlike spin correlations are favorable for the $p + ip$ -wave pairing. In that sense, for $\rho = 0.4$ where the electron density is not too low, the (short-range) antiferromagnetic order is supposed to be built and the homogeneous system exhibits $d + id$ -wave pairing. Then the onset of the hopping inhomogeneities (both the plaquette and the quasi-1D) suppresses the antiferromagnetic order and hence suppresses the $d + id$ -wave pairing. For $\rho = 0.1$, the system is supposed to harbor ferromagnetic order and hence exhibits $p + ip$ -wave pairing. However, due to the fact that the electron density is very low, the order in the system may be very weak and fragile, so the effect of the hopping inhomogeneities on the magnetic order and the pairing symmetries may be hard to predict. Our study reveals that the hopping inhomogeneities have strong effect on the pairing symmetries on the Hubbard honeycomb lattice and may be useful for the design of artificial graphene superconductors with different pairing symmetries, especially for the pursuit of the $d + id$ -wave, $p + ip$ -wave, or f -wave superconductors at low electron fillings.

ACKNOWLEDGMENTS

We thank H. M. Guo and T. Wang for useful discussions. This work is supported by the joint guiding project of Natural Science Foundation of Heilongjiang Province (Grant No. LH2019A011) and the Fundamental Research Funds for the Central Universities (Grant No. HIT.NSRIF.2019057). We thank the HEPC Studio at Physics School of Harbin Institute of Technology for access to high performance computing resources through INSPUR-HPC@hepc.hit.edu.cn.

-
- [1] K. S. Novoselov, A. K. Geim, S. V. Morozov, D. Jiang, Y. Zhang, S. V. Dubonos, I. V. Grigorieva, and A. A. Firsov, Electric field effect in atomically thin carbon films, *Science* **306**, 666 (2004).
 - [2] A. H. Castro, F. Guinea, N. M. R. Peres, K. S. Novoselov, and A. K. Geim, The electronic properties of graphene, *Rev. Mod. Phys.* **81**, 109 (2009).
 - [3] D. V. Khveshchenko, Ghost Excitonic Insulator Transition in Layered Graphite, *Phys. Rev. Lett.* **87**, 246802 (2001).
 - [4] I. F. Herbut, Interactions and Phase Transitions on Graphene's Honeycomb Lattice, *Phys. Rev. Lett.* **97**, 146401 (2006).
 - [5] C. Y. Hou, C. Chamon, and C. Mudry, Electron Fractionalization in Two-Dimensional Graphene-like Structures, *Phys. Rev. Lett.* **98**, 186809 (2007).
 - [6] C. Honerkamp, Density Waves and Cooper Pairing on the Honeycomb Lattice, *Phys. Rev. Lett.* **100**, 146404 (2008).
 - [7] S. Raghu, X. L. Qi, C. Honerkamp, and S. C. Zhang, Topological Mott Insulators, *Phys. Rev. Lett.* **100**, 156401 (2008).
 - [8] J. E. Drut and T. A. Lahde, Is Graphene in Vacuum an Insulator? *Phys. Rev. Lett.* **102**, 026802 (2009).
 - [9] Z. Y. Meng, T. C. Lang, S. Wessel, F. F. Assaad, and A. Muramatsu, Quantum spin liquid emerging in two-dimensional correlated Dirac fermions, *Nature (London)* **464**, 847 (2010).
 - [10] S. Sorella, Y. Otsuka, and S. Yunoki, absence of a spin liquid phase in the Hubbard model on the honeycomb lattice, *Sci. Rep.* **2**, 992 (2012).
 - [11] M. V. Ulybyshev, P. V. Buividovich, M. I. Katsnelson, and M. I. Polikarpov, Monte Carlo Study of the Semimetal-Insulator Phase Transition in Monolayer Graphene with a Realistic Interelectron Interaction Potential, *Phys. Rev. Lett.* **111**, 056801 (2013).
 - [12] A. M. Black-Schaffer and C. Honerkamp, Chiral d -wave superconductivity in doped graphene, *J. Phys. Condens. Matter* **26**, 423201 (2014).
 - [13] A. M. Black-Schaffer and S. Doniach, Resonating valence bonds and mean-field d -wave superconductivity in graphite, *Phys. Rev. B* **75**, 134512 (2007).
 - [14] S. Pathak, V. B. Shenoy, and G. Baskaran, Possible high-temperature superconducting state with a $d + id$ pairing symmetry in doped graphene, *Phys. Rev. B* **81**, 085431 (2010).

- [15] T. Ma, Z. Huang, F. Hu, and H. Q. Lin, Pairing in graphene: A quantum Monte Carlo study, *Phys. Rev. B* **84**, 121410(R) (2011).
- [16] R. Nandkishore, L. S. Levitov, and A. V. Chubukov, Chiral superconductivity from repulsive interactions in doped graphene, *Nat. Phys.* **8**, 158 (2012).
- [17] W. S. Wang, Y. Y. Xiang, Q. H. Wang, F. Wang, F. Yang, and D. H. Lee, Functional renormalization group and variational Monte Carlo studies of the electronic instabilities in graphene near 1/4 doping, *Phys. Rev. B* **85**, 035414 (2012).
- [18] M. L. Kiesel, C. Platt, W. Hanke, D. A. Abanin, and R. Thomale, Competing many-body instabilities and unconventional superconductivity in graphene, *Phys. Rev. B* **86**, 020507(R) (2012).
- [19] X. Y. Xu, S. Wessel, and Z. Y. Meng, Competing pairing channels in the doped honeycomb lattice Hubbard model, *Phys. Rev. B* **94**, 115105 (2016).
- [20] T. Ying, and S. Wessel, Pairing and chiral spin density wave instabilities on the honeycomb lattice: A comparative quantum Monte Carlo study, *Phys. Rev. B* **97**, 075127 (2018).
- [21] B. Uchoa and A. H. Castro Neto, Superconducting States of Pure and Doped Graphene, *Phys. Rev. Lett.* **98**, 146801 (2007).
- [22] J. P. L. Faye, P. Sahebsara, and D. Sénéchal, Chiral triplet superconductivity on the graphene lattice, *Phys. Rev. B* **92**, 085121 (2015).
- [23] X. C. Zhu, T. Ying, H. M. Guo, S. P. Feng, Quantum Monte Carlo study of the dominating pairing symmetry in doped honeycomb lattice, *Chin. Phys. B* **28**, 077401 (2019).
- [24] K. S. Novoselov, D. Jiang, F. Schedin, T. J. Booth, V. V. Khotkevich, S. V. Morozov, and A. K. Geim, Two-dimensional atomic crystals, *Proc. Natl. Acad. Sci. USA* **102**, 10451 (2005).
- [25] G. Q. Wang, M. O. Goerbig, C. Miniatura, and B. Gremaud, Emergent spin liquids in the Hubbard model on the anisotropic honeycomb lattice, *Europhys. Lett.* **95**, 47013 (2010).
- [26] T. Watanabe and S. Ishihara, Superconductivity in ionic-Hubbard model on honeycomb lattice, *Physica C: Superconductivity* **484**, 56 (2013).
- [27] H. F. Lin, H. D. Liu, H. S. Tao, and W. M. Liu, Phase transitions of the ionic Hubbard model on the honeycomb lattice, *Sci. Rep.* **5**, 9810 (2015).
- [28] H. M. Guo, T. Mendes-Santos, W. E. Pickett, and R. T. Scalettar, Magnetic order-disorder transitions on a one-third-depleted square lattice, *Phys. Rev. B* **95**, 045131 (2017).
- [29] H. Yao, W. F. Tsai, and S. A. Kivelson, Myriad phases of the checkerboard Hubbard model, *Phys. Rev. B* **76**, 161104(R) (2007).
- [30] W. F. Tsai, H. Yao, A. Lauchli, and S. A. Kivelson, Optimal inhomogeneity for superconductivity: Finite-size studies, *Phys. Rev. B* **77**, 214502 (2008).
- [31] S. Baruch and D. Orgad, Contractor-renormalization study of Hubbard plaquette clusters, *Phys. Rev. B* **82**, 134537 (2010).
- [32] T. Ying, R. Mondaini, X. D. Sun, T. Paiva, R. M. Fye, and R. T. Scalettar, Determinant quantum Monte Carlo study of d -wave pairing in the plaquette Hubbard hamiltonian, *Phys. Rev. B* **90**, 075121 (2014).
- [33] D. G. S. P. Doluweera, A. Macridin, T. A. Maier, M. Jarrell, and T. Pruschke, Suppression of d -wave superconductivity in the checkerboard Hubbard model, *Phys. Rev. B* **78**, 020504(R) (2008).
- [34] S. Chakraborty, D. Sénéchal, and A. M. S. Tremblay, d -wave superconductivity on the checkerboard Hubbard model at weak and strong coupling, *Phys. Rev. B* **84**, 054545 (2011).
- [35] H. H. Zhao, C. K. Xu, Q. N. Chen, Z. C. Wei, M. P. Qin, G. M. Zhang, and T. Xiang, Plaquette order and deconfined quantum critical point in the spin-1 bilinear-biquadratic Heisenberg model on the honeycomb lattice, *Phys. Rev. B* **85**, 134416 (2012).
- [36] P. Corboz, M. Lajko, K. Penc, F. Mila, and A. M. Lauchli, Competing states in the SU(3) Heisenberg model on the honeycomb lattice: Plaquette valence-bond crystal versus dimerized color-ordered state, *Phys. Rev. B* **87**, 195113 (2013).
- [37] P. Nataf, M. Lajko, P. Corboz, A. M. Lauchli, K. Penc, and F. Mila, Plaquette order in the SU(6) Heisenberg model on the honeycomb lattice, *Phys. Rev. B* **93**, 201113(R) (2016).
- [38] S. S. Chung and P. Corboz, SU(3) fermions on the honeycomb lattice at 1/3 filling, *Phys. Rev. B* **100**, 035134 (2019).
- [39] B. Roy and I. F. Herbut, Unconventional superconductivity on honeycomb lattice: Theory of Kekule order parameter, *Phys. Rev. B* **82**, 035429 (2010).
- [40] K. K. Gomes, W. Mar, W. Ko, F. Guinea, and H. C. Manoharan, Designer Dirac fermions and topological phases in molecular graphene, *Nature (London)* **483**, 306 (2012).
- [41] M. Polini, F. Guinea, M. Lewenstein, H. C. Manoharan, and V. Pellegrini, Artificial honeycomb lattices for electrons, atoms and photons, *Nat. Nanotechnol.* **8**, 625 (2013).
- [42] C. H. Park and S. G. Louie, Making massless Dirac fermions from a patterned two-dimensional electron gas, *Nano Lett.* **9**, 1793 (2009).
- [43] A. S. Botana, V. Pardo, W. E. Pickett, and M. R. Norman, Charge ordering in $\text{Ni}^{1+}/\text{Ni}^{2+}$ nickelates: $\text{La}_4\text{Ni}_3\text{O}_8$ and $\text{La}_3\text{Ni}_2\text{O}_6$, *Phys. Rev. B* **94**, 081105(R) (2016).
- [44] J. Zhang, Y. S. Chen, D. Phelan, H. Zheng, M. R. Norman, and J. F. Mitchell, Stacked charge stripes in the quasi-2D trilayer nickelate $\text{La}_4\text{Ni}_3\text{O}_8$, *PNAS* **113**, 8945 (2016).
- [45] R. Blankenbecler, R. L. Sugar, and D. J. Scalapino, Monte Carlo calculations of coupled boson-fermion systems, *Phys. Rev. D* **24**, 2278 (1981).
- [46] S. R. White, D. J. Scalapino, R. L. Sugar, E. Y. Loh, Jr., J. E. Gubernatis, and R. T. Scalettar, Numerical study of the two-dimensional Hubbard model, *Phys. Rev. B* **40**, 506 (1989).
- [47] E. Y. Loh, J. E. Gubernatis, R. T. Scalettar, S. R. White, D. J. Scalapino, and R. L. Sugar, The sign problem in the numerical simulation of many electron systems, *Phys. Rev. B* **41**, 9301 (1990).
- [48] S. R. White, D. J. Scalapino, R. L. Sugar, N. E. Bickers, and R. T. Scalettar, Attractive and repulsive pairing interaction vertices for the two-dimensional Hubbard model, *Phys. Rev. B* **39**, 839 (1989).
- [49] Z. Y. Weng, D. N. Sheng, and C. S. Ting, Large-U Hubbard model: the crossover from one dimension to two dimensions, *Phys. Lett. A* **175**, 455 (1993).
- [50] U. Ledermann, Dimensional crossover in half-filled and lightly doped N -leg Hubbard ladders, *Phys. Rev. B* **64**, 235102 (2001).
- [51] Y. F. Kung, C. Bazin, K. Wohlfeld, Y. Wang, C.-C. Chen, C. J. Jia, S. Johnston, B. Moritz, F. Mila, and T. P. Devereaux, Numerically exploring the 1D-2D dimensional crossover on spin dynamics in the doped Hubbard model, *Phys. Rev. B* **96**, 195106 (2017).